Flow Induced Vibration of a microvalve for aerodynamic control

Olivier DUCLOUX, Karim TALBI, Leticia GIMENO, Romain VIARD, Philippe PERNOD, Vladimir PREOBRAZHENSKY

Joint European Laboratory on Nonlinear Magnetoacoustics of condensed matter (LEMAC) : Institute of Electronics, Microelectronics and Nanotechnology (IEMN DOAE UMR CNRS 8520) Ecole Centrale de Lille, B.P. 48, 59651 Villeneuve d'Ascq Cedex, France

Alain MERLEN

Joint European Laboratory on Nonlinear Magnetoacoustics of condensed matter (LEMAC)

Laboratory of Mechanics of Lille (LML UMR CNRS 8146) University of Lille 1, 59655 Villeneuve d'Ascq Cedex, France

ABSTRACT

The reattachment of separated air flows can be actively controlled by blowing oscillatory air jets in the boundary layer, through submillimetric holes. Performance improvement of the next generation planes (lift enhancement, drag reduction,…) pushes plane designers to investigate MEMS solutions in order to provide active control of the air flow surrounding wings and compressor blades. In order to answer the needs of the aeronautical industry, several microjet technologies were developed these last years [1]. In this paper, we present a small sized, high flow rate, dynamically actuated microvalve designed to provide pulsed jets without energy supply. The pulsed jet is obtained by an oscillation of the valve induced by an interaction between a flexible structure and the flow in the inlet channel. The micro-valves were fabricated and characterized.

1. INTRODUCTION

Recent advances in fluid mechanics have shown the possibility to control detached flows with the blowing of pulsed gas microjets through submillimetric holes located slightly upstream the detachment bubble (see for example Wygnanski 1997). In the case of aeronautical applications like in Erbsloeh et al 2004, the active control of the flow around wings, compressor blades, and intake may provide lift enhancement, drag, consumption reduction, etc. To provide such jets, microelectromechanical systems (MEMSs_) are currently investigated for their high integrability and low power consumption.

The aimed performances are an outlet microjet speed higher than 100 m/ s and a minimum pulsation frequency of 1 kHz. Much work has recently been done as in (Ho et al 1998, or Pernod et al 2006) on the design and fabrication of suitable systems.Microvalve solutions based on electrostatic, (Frutos et al 2005) piezoelectric, (Warsop 2004) or magnetostatic (Ducloux et al 2006) actuation techniques provide either acceptable actuation frequency or outlet speed. In this letter, we present a microvalve design allowing a 2 kHz pulsation of a 100 m/ s microjet with no electric energy supply. The actuation is

based on the self-oscillation of a mobile rigid pad located over a flexible membrane originated by the pressure drop in the fluid flowing under the moving part. The physical mechanism of the observed auto-oscillation is described and confirmed experimentally.

2. THE MICROSYSTEM

The MEMS architecture under consideration consists of a silicon microchannel covered with a flexible polydimethylsiloxane (PDMS) membrane (60 μm thickness). A rigid pad, processed over the membrane, is free to move upward or rotate under the effect of the pressure distribution introduced

by a series of four silicon walls processed in the microchannel under the pad (Figure. 1). The actuation is obtained by mechanical pinching of the silicon microchannel via the rigid pad movement. Outlet speed and actuation frequencies are determined by the inlet pressure P_{in} and the geometrical characteristics of the microchannel.

Such a device is fabricated using conventional microfabrication techniques. It consists in the stacking of three independently processed silicon wafers subsequently bonded together: two for the micro-channel part, and one for the micro-membranes (Figure 2).

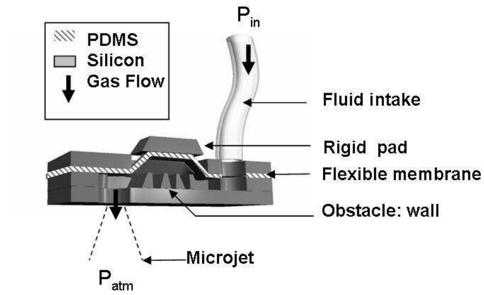

Figure. 1: *Microvalve architecture.*

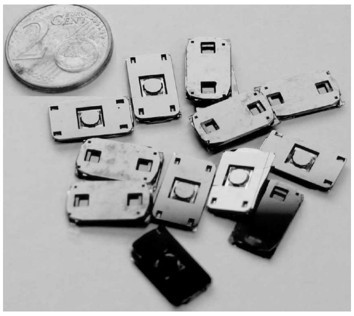

Figure. 2: *Microvalves*

3. THEORETICAL ANALYSIS

We assume that two variables describe the rigid pad movement: H defines the vertical displacement of the centre of the pad, and θ its rotational movement in the plane (O,x,y). Other geometrical constants are defined in figure 2. The rigid pad is affected by the inner pressure and the tensile stress induced in the membrane by the pad displacement. In order to simplify the model, the pressure distribution is supposed constant on each half of the mobile pad. The resulting pressure forces F_{P1} and F_{P2} are associated to pressures P_1 and P_2.

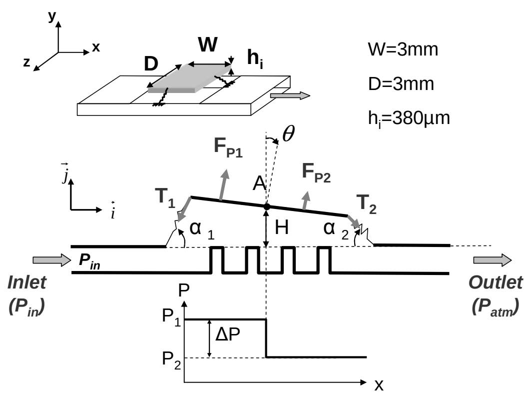

Figure 3: *Notations and dimensions*

The next step consists in a static analysis of the membrane deflection under the effect of the inner pressure. Static displacement and rotation of the pad (H_0 , θ_0), are determined as a function of the inlet pressure by direct measurement using a low focus length microscope (focus x 150): focus is made on each side of the pad, the perpendicular adjustment of the microscope corresponding to the pad perpendicular movement. The obtained measurements are then approximated using 3rd order polynomials. Static solutions (H_0, θ_0) and approximations are shown in figure 3.

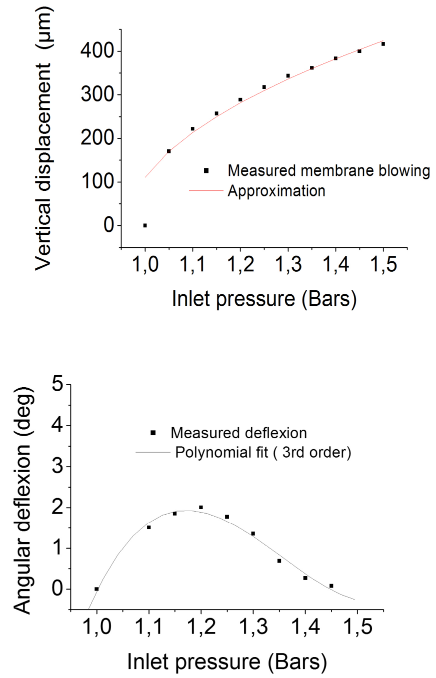

Figure 4: *Measured static deformations H_0 and θ_0 as a function of the inlet pressure Pin. $H_0(P_{in})$ and $\theta_0(P_{in})$ are approximated using polynomial functions.*

The next step is a dynamical analysis of the pad movement around the static position $H_0(P_{in})$,$\theta_0(P_{in})$. The control parameter is the pressure drop under the membrane. An analytical determination of this pressure drop under the membrane is impossible because of the complexity of the microchannel geometry. For this reason, the pressure distribution under the membrane obtained by a numerical simulation of the compressible 3D Navier-Stokes equations with k-ε turbulence model (Reynolds number of 3800). In order to simplify the dynamical system, the pressure distribution is averaged on each half of the mobile pad to obtain the resulting pressures $P_1(H,\theta)$ and $P_2(H,\theta)$. For the dynamical analysis, stationary assumption is accurate since the characteristic time corresponding to a fluid particle passing under the membrane (30 µs) is small compared to the vibration period (0.5 ms). Fonctions $P_1(H,\theta)$ and $P_2(H,\theta)$ are therefore evaluated for discrete static positions (H,θ) of the rigid pad. an finally approximated by separation of the variable:

$$P_1(H,\theta) = P_{1H}(H).p_{1\theta}(\theta)$$

$$\Delta P(H,\theta) = P_1(H,\theta) - P_2(H,\theta) = \Delta P_H(H).\Delta p_\theta(\theta)$$

Functions $p_{1\theta}$ and Δp_θ are dimensionless functions normalized, respectively, by the maximum value of $P_1(H_0,\theta_0)$ and $\Delta P(H_0,\theta_0)$ for H_0,θ_0 corresponding to $1<P_{in}<1.5$ bars. All these functions are then approximated using third-order polynomials.

Two equations of motion for the mobile silicon pad are obtained:

$$I\frac{d^2\theta}{dt^2} = D\frac{W^2}{8}\Delta P_H(H)\Delta P_\theta(\theta) - \frac{W}{2}M(H,\theta) \qquad (1)$$

with :

$$M(H,\theta) = T_1\sin(\alpha_1-\theta) - T_2\sin(\alpha_2-\theta) = A(H).\theta + o(\theta^2)$$

and

$$m\frac{d^2H}{dt^2} = D\frac{W}{2}(2P_{1H}(\theta)P_{1\theta}(\theta) - \Delta P_H(H)\Delta P_\theta(\theta)) - F(H,\theta) \qquad (2)$$

with:

$$F(H,\theta) = T_1\sin(\alpha_1) + T_2\sin(\alpha_2) = B(H).H + o(\theta^2)$$

where T_1, T_2 are the tensions of the membrane and angles α_1, α_2 and length W, D are defined in figure 3. *I* and *m* are respectively the inertia and the mass of the pad. Functions A and B are obtained developments of first order in $\theta<<1$.

Taking advantage of the small displacement method around the static solution (H_0,θ_0), new variables are defined by: $H = H_0 + h$, and $\theta = \theta_0 + \phi$ with $h/H_0 << 1$ and $\phi/\theta_0 <<1$.

Equations (1) and (2) can be reduced to the quasi-linear coupled system of equations:

$$\frac{d^2h}{dt^2} = -\omega_H{}^2 h + \xi\phi \text{ and } \frac{d^2\phi}{dt^2} = -\omega_\theta{}^2\phi - \eta h \qquad (3)$$

where ω_H, ξ, ω_θ and η are given in Ducloux et al (2007). Assuming the solution to be harmonic, one can find the eigen frequency of the system from the dispersion equation :

$$\omega^4 - \omega^2(\omega_\theta{}^2 + \omega_H{}^2) + \omega_\theta{}^2\omega_H{}^2 + \eta\xi = 0 \qquad (4)$$

Figure 5 shows the calculated solutions $f_1 = \omega_1/2\pi$ and $f_2 = \omega_2/2\pi$ of eq. (4) as functions of the inlet pressure P_{in} that determined the static position $H_0(P_{in})$, $\theta_0(P_{in})$. Real parts of f_1 and f_2 match in the P_{in} range [1.17 Bars , 1.4 Bars]. A non nil imaginary part of the solutions corresponds to unstable states (H_0,θ_0).

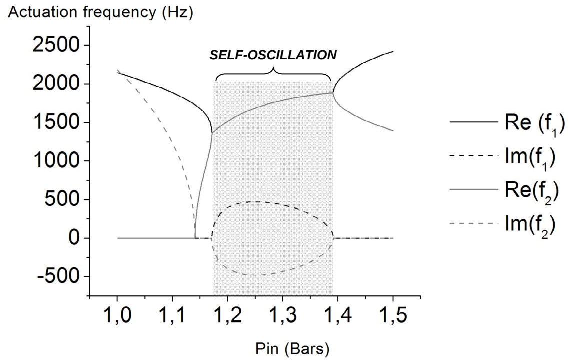

Figure 5: *Calculated actuation frequencies. Presence of a self-oscillation range depending on the inlet pressure.*

In the area $P_{in}<1.15$ bars, the instability means that the value of the pressure P_{in} is not important enough to maintain the valve opened.

The area 1.17 bars$<P_{in}<$1.41 Bars corresponds to the self-oscillations with the frequency equal to $Re(f_2)$. The negative value of $Im(f_2)$ means that the amplitude grows exponentially. Of course this is due to the linearity of system 3. It shows that the self-oscillation reaches quickly a high amplitude but cannot predict the saturation level in such quasi-linear approach. Nevertheless the model provides the actuation frequency as a function of the geometrical characteristics of the microchannel and micromembrane. For $P_{in}>$ 1.41 bars, the imaginary parts are zero, but non nil real frequencies exist. This means that the valve cannot oscillate spontaneously if they are not shifted from they equilibrium position.

4. EXPERIMENTAL VALIDATION

The characterization of the valve performances is obtained by direct measurement of the outlet microjet speed. This measurement is undertaken using a 55P11 DANTEC hot wire anemometer (Brunn 1995) (length 1.25 mm, diameter 5 µm) presented figure 6. The measuring probe is fixed at 500 µm away from the outlet hole, and oriented parallel to the microjet axis using a 3-axis micro-positioning setup. Measurements of the actuation frequency in the self-oscillation mode presented in figure 7 show a good agreement between the calculated and measured values as a function of the inlet pressure. The measured oscillations t are detected in the range [Pin=1.1 Bars, pin=1.36 Bars]. For Pin>1.36 Bars, the microvalves stop self-oscillating and need an external mechanical impulsion to be able to oscillate again. Physically, this result can be explained by the weakness of the remaining mechanical coupling between the moving part and the fluid when the membrane is very extended by the high inlet pressures.

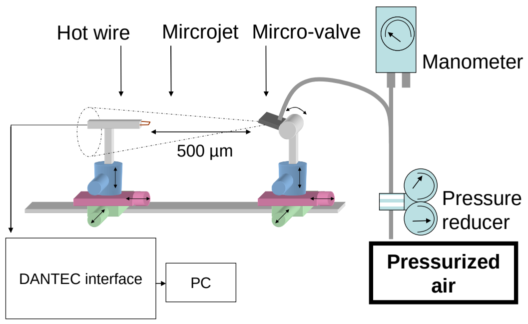

Figure 6: *Experimental setup.*

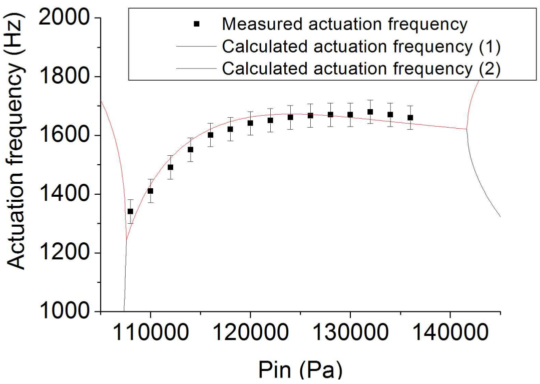

Figure 7: *Experimental frequency versus P_{in}.*

In order to show the strong dependency between the geometrical characteristics of the microvalves and the self oscillation phenomena, a second microchannel geometry with only two walls at the bottom of the channel was fabricated and studied. In that case the pressure distribution under the membrane in open mode was then quasihomogenous. For this reason, both experimental and theoretical results show no self-oscillation, as the coupling between the pressure drop and the membrane position is too low.

5. CONCLUSION

The fluid-structure self-oscillation phenomenon studied in the present paper was used for the actuation of a microvalves of high flow rate and high actuation frequency dedicated to flow control applications. Measured microjet characteristics are up to 150 m/ s outlet speed actuated at 2 kHz with no specific energy supply. The theoretical analysis of the problem, combined with Navier-Stokes numerical simulation and experimental validation, provides the relevant physical parameters for the geometrical characteristics of the mobile pad and silicon walls. So, the results can be transposed to fit the performances to the specific requirement of the applications. A set of such microvalves was installed in an anechoic wind tunnel on the rear part of a high speed jet in order to experiments its effects on the aeroacoustic properties of the jet. (Figure 8 and 9)

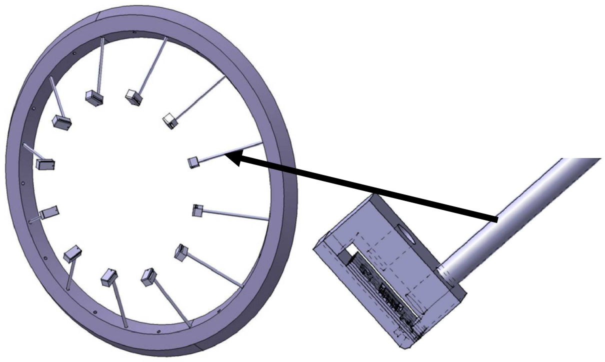

Figure 8: *Packaging of the self-oscillating valves around a high speed jet.*

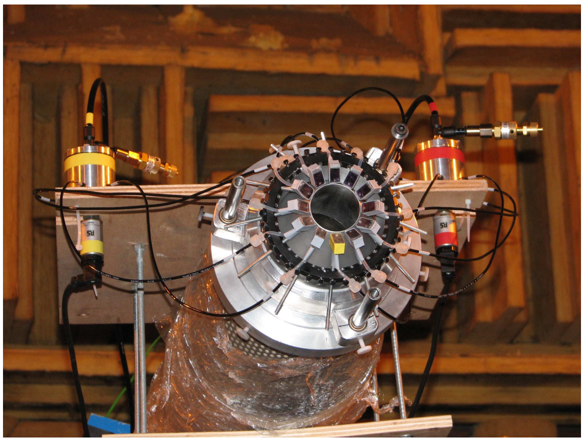

Figure 9: *View of the microvalves inside an anechoic wind tunnel*

6. REFERENCES

Wygnanski, I., 1997, Boundary layer and flow control by periodic addition of momentum”, AIAA Paper 97-2117.

Erbsloeh, S., Crowther, W. J., Frutos, J. R., 2004 Control of boundary layer separation on a civil turbofan intake using air jet vortex generators, 2nd AIAA Flow Control Conference.

Ho, C., M., Tai, Y.C., 1998, MicroelectroMechanical Systems (MEMS) and fluid flows”, Ann. Rev. Fluid. Mech., 30, 602-609.

Pernod, P., Preobrazhensky, V., Merlen, A., Ducloux, O., Talbi, A., Gimeno, L., Tiercelin, N., 2006, Proc. IUTAM symposium on flow control and MEMS, London, in Flow control and MEMS, J. Morrison et al. (Eds.), Springer, Dordrecht, 2008

Frutos, J. R., Vernier, D., Bastien,, F., de Labachelerie, M., Bailly, Y., 2005, IEEE Sensors, 7, 30.

Warsop, C., 2004, Aeromems a european research effort to develop mems based on flow control technologies, Proc. AIAA 2nd Flow Control Conference.
.
Ducloux, O., Deblock,Y., Talbi, A., Pernod, P., Preobrazhensky, V.,Merlen, A., 2006 Proc. IUTAM symposium on flow control and MEMS, London, in Flow control and MEMS, J. Morrison et al. (Eds.), Springer, Dordrecht, 2008

Ducloux, O., Talbi, A., Gimeno, L., Viard, R., Pernod, P., Preobrazhensky, V., Merlen A., 2007 Self-oscillation mode due to fluid-structure interaction in a micromechanical valve Appl. Phys. Let.91 (3) art 024101

Bruun, H.H., 1995, Hot wire anemometry: principles and signal analysis, Oxford University Press, New York,